frontiers | Frontiers in Earth Science

TYPE Original Research
PUBLISHED 20 January 2023
DOI 10.3389/feart.2022.1059838

OPEN ACCESS

EDITED BY
Wenlong Ding,
China University of Geosciences, China

REVIEWED BY
Xiaoping Liu,
China University of Petroleum, Beijing, China
Chin Yik Lin,
University of Malaya, Malaysia

*CORRESPONDENCE
Haizhou Qu,
quhaizhou@swpu.edu.cn

SPECIALTY SECTION
This article was submitted to Structural Geology and Tectonics, a section of the journal Frontiers in Earth Science

RECEIVED 02 October 2022
ACCEPTED 21 November 2022
PUBLISHED 20 January 2023

CITATION
Zou B, Qu H, Zhao R, Zhang L, Zhang Y, Ma Z, Zhang X, Huang Q, Mo Q, An H and Pei Y (2023), Diagenesis of the first member of Canglangpu Formation of the Cambrian Series 2 in northern part of the central Sichuan Basin and its influence on porosity.
Front. Earth Sci. 10:1059838.
doi: 10.3389/feart.2022.1059838

Diagenesis of the first member of Canglangpu Formation of the Cambrian Series 2 in northern part of the central Sichuan Basin and its influence on porosity

Bing Zou[1,2], Haizhou Qu[1,2]*, Rongrong Zhao[3], Lianjin Zhang[4], Yu Zhang[3], Zike Ma[4], Xingyu Zhang[1,2], Qinyang Huang[1,2], Qianwen Mo[3], Hongyi An[3] and Yu Pei[5]

[1]State Key Laboratory of Oil and Gas Reservoir Geology and Exploitation, Southwest Petroleum University, Chengdu, China, [2]School of Geoscience and Technology, Southwest Petroleum University, Chengdu, China, [3]Exploration Department of PetroChina Southwest Oil and Gasfield Company, Chengdu, China, [4]Central Sichuan Oil and Gas Mine of PetroChina Southwest Oil and Gas Field Company, Suining, China, [5]Geological Exploration & Development Research Institute, CNPC Chuanqing Drilling Engineering Company Limited, Chengdu, China

In this paper, taking the first Member of the Canglangpu Formation of the Cambrian Series 2 in the northern central Sichuan Basin as an example, the diagenesis and its influence on porosity are systemically studied based on the observations and identifications of cores, casts and cathodoluminescence thin sections. The results show that the rock types of the first member of Canglangpu Formation are various, including mixed rocks, carbonate rocks and clastic rocks. The specific lithology is dominated by sand-bearing oolitic dolomite, sandy oolitic dolomite, sparry oolotic dolomite and fine-grained detrital sandstone. At the same time, the Cang 1 Member has experienced five types of diagenetic environments, including seawater, meteoric water, evaporative seawater, shallow burial, and medium-deep burial diagenetic environments. Moreover, the main diagenetic processes under different diagenetic environments include cementation, dissolution, compaction, chemical compaction, dolomitization and structural fractures. According to the analysis, fabric-selective dissolution in meteoric water diagenetic environment, dolomitization in evaporative seawater environment, and non-fabric-selective dissolution, dolomitization and structural fractures in buried diagenetic environment are beneficial to the development of pores. However, cementation, compaction and chemical compaction in medium and deep burial environments, are unfavorable for the development of pores.

KEYWORDS

diagenesis, Series 2, Cambrian, the first member of Canglangpu Formation, northern part of the Central Sichuan Basin

1 Introduction

The Central Sichuan Paleo-uplift controls the process of hydrocarbon accumulation in the Sinian-Cambrian Series 2 in the Sichuan Basin. At present, the exploration horizons in this area are mainly concentrated in the Sinian Dengying Formation and the Cambrian Series 2 Longwangmiao Formation, and there are few studies on other horizons. Until Well JT1 in the northern part of the central Sichuan Basin encountered thick dolomite in the Cang 1 Member, and industrial gas flow of 51.62 × 10^4 m^3/d was obtained (Yue et al., 2020), proving that the Canglangpu Formation has great hydrocarbon exploration potential. According to previous studies, shelf, coastal, platform, tidal flat, slop and delta facies are developed in the Cang 1 Member in the study area (Peng et al., 2020; Yan et al., 2020; Ma et al., 2021; Li et al., 2021a; Wang et al., 2022). Influenced by the Kangdian Ancient Continent in the west and the Chengguan complex rock masses in the northwest part, a set of "mixed sediments" of interbedded terrigenous clasts and carbonate rocks were deposited in the Cang 1 Member of the Canglangpu Formation (Yan et al., 2020). In a broad sense, mixed sediments refer to the mixing of terrigenous clastic and carbonate components in the same rock layer and the mixing of interbedded clastic and carbonate rocks (Zhang and Ye, 1989; Sha, 2001; Li et al., 2021b). At present, many previous studies have been carried out on the lithology identification, sedimentary facies, sequence stratigraphy and reservoir properties of the Canglangpu Formation in the study area (Wang et al., 2018; Peng et al., 2020; Wen et al., 2020; Yan et al., 2020; Li et al., 2021a; Dong et al., 2021; Ma et al., 2021; Yan et al., 2021; Li et al., 2022a; Wang et al., 2022), but there is no report on the diagenesis of the Cang 1 Member of the Canglangpu Formation and its influence on porosity. Thus, this paper will study the diagenesis of the Cang 1 Member of the Canglangpu Formation and its influence on porosity.

2 Geological background

The Sichuan Basin lies within the Middle and Upper Yangtze Craton and is a sedimentary basin bounded by folds and faults. The study area is located in the northern part of the central Sichuan Basin. It is located in the gentle tectonic zone of the central Sichuan Basin (Figure 1A) (Hu et al., 2021). The Canglangpu Formation is called "lower red bed" (Wang et al., 2014). According to its lithologic types and lithologic assemblages, the Canglangpu Formation can be divided into the Cang 1 and Cang 2 Members. During the Cang 1 Member period, the clastic and carbonate rocks were mainly developed on

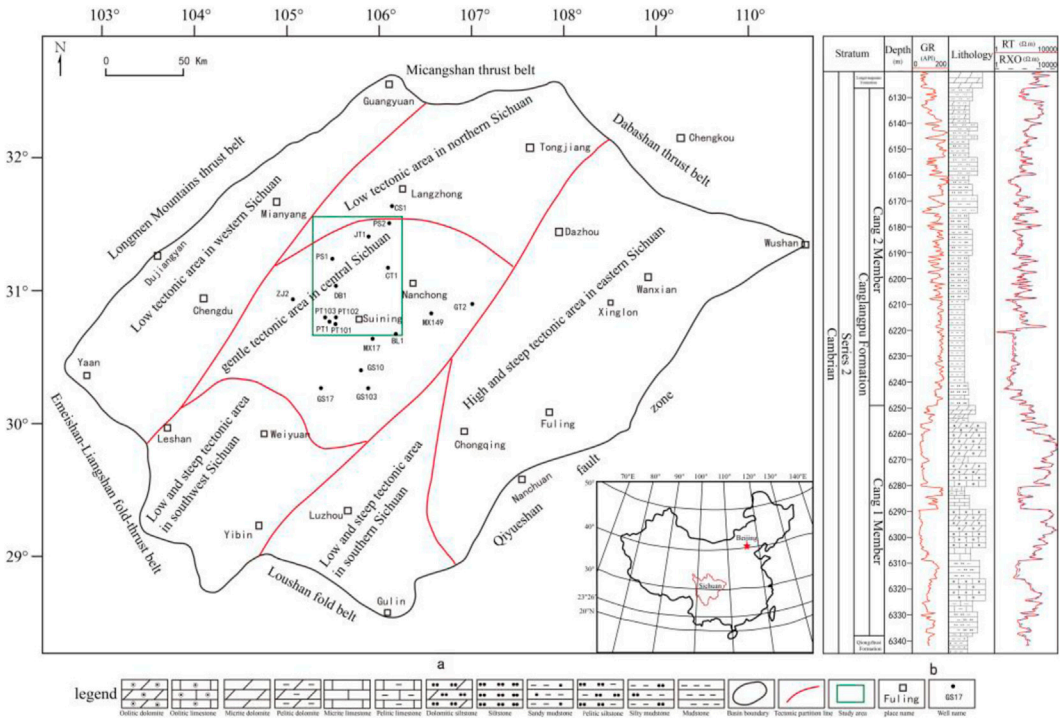

FIGURE 1
Location and comprehensive stratigraphic histogram of the study area. **(A)** Structural unit division of the Sichuan Basin (modified from Reference Hu et al., (2021)); **(B)** Lithologic histogram of the Canglangpu Formation in Well CT1. GR: natural gamma ray; Rt: true formation resistivity; Rxo: flushed zone formation resistivity.

the west side of the Deyang-Anyue Rift Trough, while the carbonate rocks were mainly developed on the east side. During the Cang 2 Member period, the rifting trough was filled up, and clastic rocks were mainly deposited (Yan et al., 2020) (Figure 1B).

3 Samples and methods

Cores from Wells CT1, PS1, PS2, PT101 and DB1 in the study area are selected for core observations. 10% HCl was used to identify calcite and dolomite in the cores. At the same time, a total of 147 thin sections were prepared from cores that sampled uniformly from five Wells (CT1, PS1, PS2, PT101 and DB1). Alizarin red S and potassium ferricyanide were used to stain thin sections, and an EISS microscope (model: AXIO Scope. A1) was used to distinguish dolomite, calcite, ferric dolomite, and ferric calcite. Observations and identifications of lithology and analysis of the diagenetic process of the Cang 1 Member are the basis of the restoration of diagenetic processes. Then, 21 thin sections with well-developed cements were selected from 147 thin sections. The lithology mainly includes sand-bearing oolitic dolomite, sandy oolitic dolomite, sparry oolitic dolomite, sparry oolitic limestone and fine-grained lithic sandstone. Cathodoluminescence microscope (model: CL 8200 MK5) was used. When the voltage was 9–11 V, the exposure time was adjusted to about 3 s. The luminescence characteristics of various rock components were observed, and the stages of cements were distinguished. Combined with the characteristics of diagenesis, the diagenetic stage, diagenetic environment and diagenetic sequence were divided.

4 Results

4.1 Petrological features

The rock types of the target layer are mainly include mixed rocks, carbonate rocks and clastic rocks.

4.1.1 Mixed rocks

At present, the classification of mixed rocks has not been unified. Its classification scheme was first proposed by Mount (1984), and four end members of terrigenous clasts, dissimilar grains, stucco and argillaceous clay were selected to classify peperite. After that, Zhang (2000) defined mixed sediments with a carbonate content of 5%–95% and terrigenous clastic content of 5%–95% as peperite; Dong et al., 2007 classified rocks containing both terrigenous clasts and carbonate components as mixed rocks (0% < terrigenous clastic content <100%, 0% < carbonate content <100%); Yang and Sha, 1990 classified mixed sediments with carbonate composition >25% and terrigenous clast >10% as mixed rocks.

In this paper, Zhang's classification scheme of mixed rocks, that widely adopted by researchers, is used. That is, mixed sediments with carbonate content of 5%–95% and terrigenous clastic content of 5%–95%, called peperite. The mixed rocks types of the target layer in the study area mainly include sand-bearing oolitic dolomite, sandy oolitic dolomite and a small amount of sand-bearing oolitic limestone and sandy oolitic limestone.

Sand-bearing (sandy) oolitic dolomite: The terrigenous clastic particles are mainly sand-grade quartz, detritus, and a very small amount of feldspar. The particle size is 0.05–0.6 mm, and concentrated in 0.1–0.25 mm, and fine sand is dominant. The particles are sub-angular-sub-round with moderate roundness. In addition, the oolites have a particle size of 0.3–1 mm and are concentrated at 0.5–1 mm. Strong dolomitization occurs inside the oolites, and the powder-fine-grained metasomatic dolomite grains are usually in point contacts or line contacts (Figures 2A,B).

Sand-bearing (sandy) oolitic limestone: The terrigenous clastic particles are mainly terrigenous quartz and lithic debris. Its particle size is distributed in 0.05–0.3 mm, and concentrated in 0.1–0.25 mm. Fine sand is predominant, and the particles are sub-angular-sub-round with moderate roundness. In addition, the particle size distribution of oolites is 0.15–0.6 mm, and concentrated in 0.3–0.5 mm. The oolites are dominated by radial oolis, with a small amount of epidermal and oval oolites (Figure 2C).

4.1.2 Carbonate rocks

The carbonate rocks have a terrigenous clastic content less than 5% and a carbonate content more than 95%. Moreover, they are mainly composed of sparry oolitic dolomite and a small amount of sparry oolitic limestone, silty crystalline dolomite and limestone-dolomite transition rocks.

Sparry oolitic dolomite: The particles are mainly oolitic, with small amounts of terrigenous detritus (such as quartz and rock debris) and biodetritus (such as crinoids and trilobites). Among them, the content of terrigenous clasts and bioclasts are both less than 5%. In addition, there are also a small amount of sand clasts locally. The particle size distribution of the oolites is 0.3–1 mm, and they are concentrated at 0.5–1 mm. Strong dolomitization occurs inside the oolites, and polycrystalline or residual oolites are easily found (Figures 2D,E). In addition, small amounts of crinoids stems and trilobite fragments were seen as cores of oolites or as separate granules. Among them, the stems of crinoids usually have a lath-like shape, and they have a single-structure (Figure 2D); whereas, trilobites have a curved morphology and a wavy extinction structure.

Sparry oolitic limestone: The grains are mainly oolites, followed by a small amount of terrigenous quartz and detritus, the content of which is less than 5%. The particle size of the oolites is 0.2–1.5 mm, and the distribution is concentrated at 0.5–1 mm. Oolites are mostly spherical, while

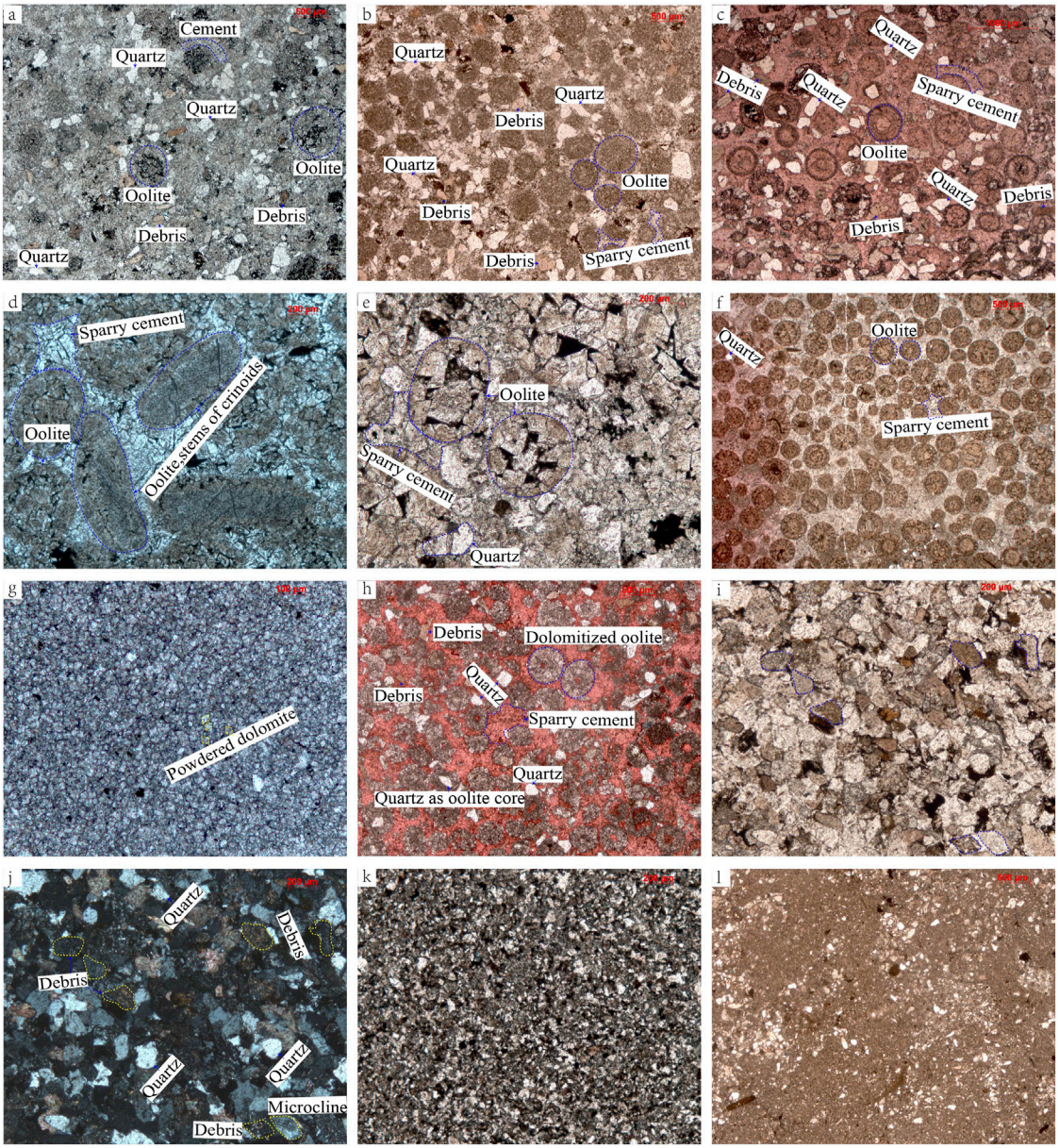

FIGURE 2
Microscopic structural features of the rock in the target layer. **(A)** Sand-bearing oolitic dolomite, Well DB1, 5942.7 m, single polarized, dyed cast thin section; **(B)** Sandy oolitic dolomite, Well PS1, 6784.21 m, single polarized light, dyed cast thin section; **(C)** Sand-bearing limestone, Well CT1, 6299.5 m, single polarized light, dyed cast thin section; **(D)** Sparry oolitic dolomite, Crinoid stems can be seen occasionally, Well DB1, 5915.7 m, single polarized, dyed cast thin section; **(E)** Sparry oolitic dolomite, Well CT1, 6273.18 m, single polarized light, dyed cast thin section; **(F)** Sparry oolitic limestone, Well CT1, 6301.31 m, single polarized light, dyed cast thin section; **(G)** powder dolomite, Well PS1, 6779.41 m, single polarized, dyed cast thin section; **(H)** Dolomite oolitic limestone, Well PS2, 7303.88 m, single polarized light, dyed cast thin section; **(I)** Fine-grained detrital sandstone, Well PT101, 5024.38m, single polarized light, dyed cast thin section; **(J)** Cross-polarized light image of sample i; **(K)** Siltstone, Well PS1, 6777.82 m, single polarized light, dyed cast thin section; **(L)** Silt mudstone, Well DB1, 5950.7 m, single polarized light, dyed cast thin section.

a few are oval. Oolites are mainly normal oolites with a core thickness greater than that of the concentric layers. A small number are epidermal oolite with a core thickness smaller than the concentric layers and oval oolis with an oval shape. In addition, cracks are developed on the surface of the oolites (Figure 2F).

Powder dolomite: The grain size distribution is in the range of 0.005–0.1 mm, and the grains are mainly composed of powder

TABLE 1 Rock characteristic of the first member of Canglangpu Formation.

Lithology	Characteristics of terrigenous detritus					Characteristics of carbonate components			
	Terrigenous particles			Argillaceous content (%)	Dolomite content (%)	Calcite content (%)	Oolite		
	Conten (%)	Main particle size (mm)	Sorting and rounding				Main types	Main particle size (mm)	Crystal content (%)
Sand-bearing (sandy) oolitic dolite	5–25 (25–50)	0.1–0.25	Well, moderate	0	5–95	0	Polycrystalline oolite, Residual oolitic	0.5–1	0
Sand-bearing (sandy) oolitic limestone	5–25 (25–51)	0.1–0.26	Well, moderate	0	0	5–95	Radial oolitic	0.3–0.5	0
Sparry oolitic dolomite	0–5	/	/	0	90–100	0–5	Radial oolitic	0.5–1	0
Sparry oolitic limestone	0–5	/	/	0	0–5	90–100	radioactive oolitic	0.5–1	0
Powder crystal dolomite	0–5	/	/	0–5	90–100	0	/	/	90–100
Dolomitic oolitic limestone	0–5	/	/	0	25–50	45–75	Polycrystalline oolite, Residual oolitic	0.2–0.5	0
Lime oolitic dolomite	0–5	/	/	0	45–75	25–50	Polycrystalline oolite, Residual oolitic	0.2–0.5	0
Fine grained lithic sandstone	90–100	0.1–0.25	well、moderate	0–10	/	/	/	/	/
Siltstone	90–100	0.01–0.1	/	0–10	/	/	/	/	/
Silty mudstone	25–50	0.01–0.1	/	50–75	/	/	/	/	/

crystal-grade dolomite. Moreover, the grains mostly have rhombic or square morphologies (Figure 2G).

Dolomitic oolitic limestone (Limestone oolitic dolomite): Dolomitization occurs inside the oolites, while there is weak dolomitization between the oolites. The oolites after dolomitization are mostly polycrystalline oolites composed of multiple powder-fine-grained dolomite crystals. In addition, a small number of oolites without dolomitization were mostly normal oolites (Figure 2H).

4.1.3 Clastic rocks

It refers to clastic rocks with terrigenous clastic content greater than 95% and carbonate content less than 5%. The main lithologies include fine-grained detrital sandstone and a small amount of siltstone and silty mudstone.

Fine-grained detrital sandstone: The detrital grains are mainly terrigenous quartz and detritus, with a very small amount of feldspar grains. Among them, the content of terrigenous quartz is 50%–60%, and the content of debris is 30%–50%. The particle size of the debris particles is 0.05–0.5 mm, and the content of the debris particles with a particle size in the range of 0.1–0.25 mm accounts for 80% of the total particle size. In addition, the particles of fine-grained detrital sandstones were mostly sub-angular-sub-round with moderate roundness (Figures 2I,J).

Siltstone: The detrital grains are mainly composed of silt-grade terrigenous quartz and detritus. The particle size is mainly distributed in 0.01–0.1 mm. Moreover, the particle size of a small amount of terrigenous quartz is larger than 0.1 mm, but its proportion is less than 10%. The silt fraction had good sorting and poor roundness (Figure 2K).

Silty mudstone: The detrital particles are mainly silt-grade terrigenous quartz and lithic debris, and their content is between 25% and 50%. The particle size is mainly 0.005–0.1 mm. In addition, its matrix is mainly brown terrigenous mud, and the content is usually between 50% and 75% (Figure 2L).

Through microscopic observation of the above lithology, the microscopic characteristics of each lithology are summarized in detail (Table 1), including the content of carbonate components and terrigenous clastic components, the sorting, rounding and particle size of terrigenous clastic particles, and the type and particle size of oolites.

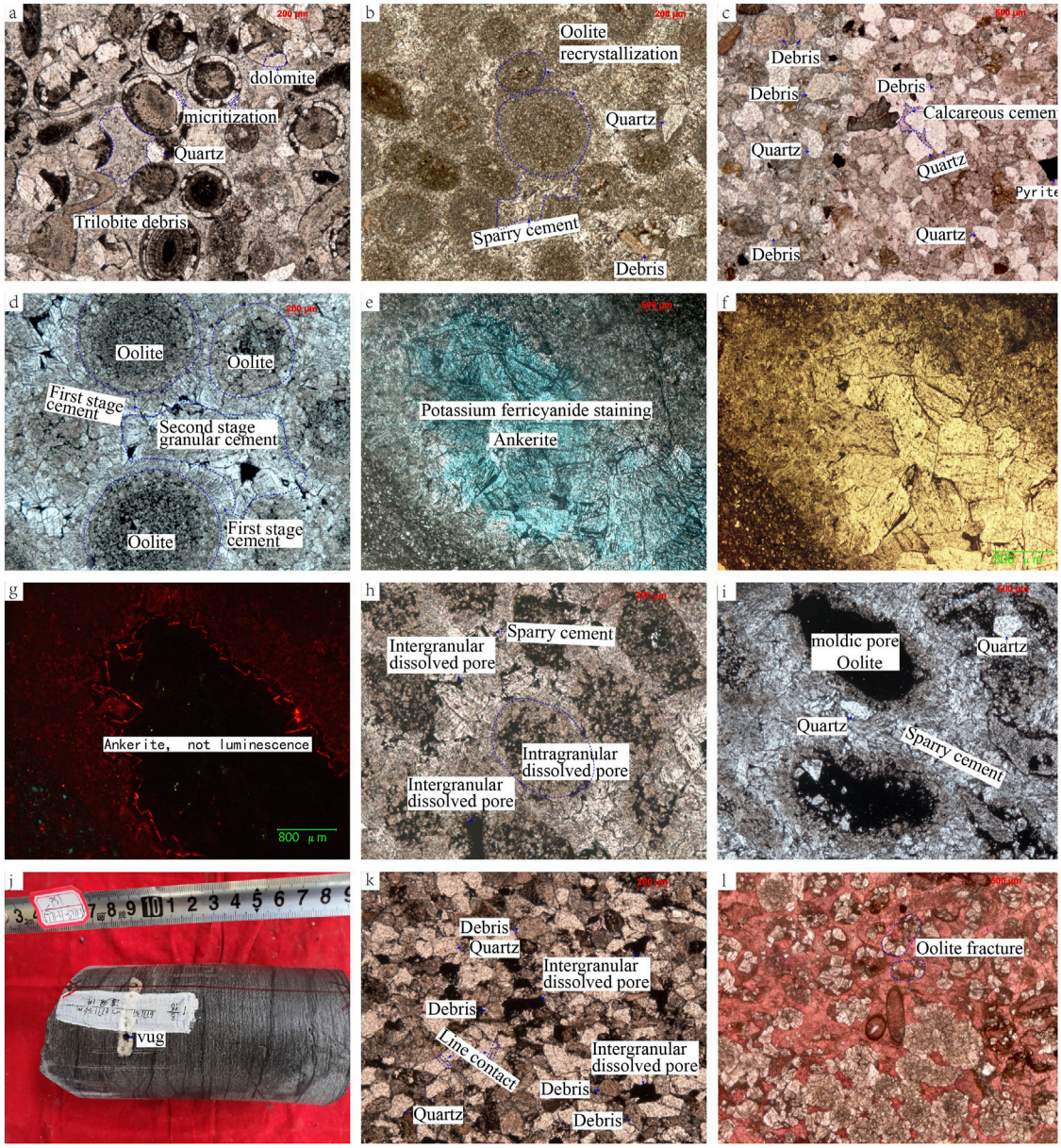

FIGURE 3
Developmental characteristics of typical diagenesisin the study area. **(A)** Micritic sleeves formed by micritization. Dolomite sparry oolitic limestone, Well CT1, 6275.63 m, single polarized light, dyed cast thin section; **(B)** Weak recrystallization occurs inside the oolites. Sparry oolitic dolomite, well PT101, 5018.1 m, single polarized light, dyed cast thin section; **(C)** Calcareous cementation at the edges of quartz grains. Calcareous fine-grained detrital sandstone, Well PT101, 5023.14 m, single polarized light, dyed cast thin section; **(D)** Horse tooth-like cement and granular cement. Sparry oolitic dolomite, Well DB1, 5938.9 m, single polarized light, dyed cast thin section; **(E)** The second phase of ankerite cement. Argillaceous silty dolomite, Well DB1, 5951.7 m, single polarized light, potassium ferricyanide dyed thin section; **(F)** Unstained thin section of sample e; **(G)** Cathodoluminescence image of sample e, the second phase ankerite cement does not emit light; **(H)** Intergranular dissolution (yellow arrows) and intragranular dissolution pores (red arrows) formed by dissolution. Sparry oolitic dolomite, CT1 well, 6264.53 m, single polarized light, dyed cast thin section; **(I)** Mold pores formed by dissolution. Sparry oolitic dolomite, Well CT1, 6268.9 m, single polarized light, dyed cast thin section; **(J)** Pores formed by dissolution, and they are mostly half filled with calcite. Gray sand-bearing oolitic dolomite, Well PS1, 6771.31–6771.56 m, core photo; **(K)** Intergranular pores formed by dissolution. Fine-grained detrital sandstone, Well DB1, 5913.45 m, single polarized light, dyed cast thin section; **(L)** Oolitic broken dolomitic oolitic limestone. Well CT1, 6285.76 m, single polarized, dyed cast thin section.

4.2 Diagenesis process

4.2.1 Diagenesis types and characteristics

According to the microscopic observation results, the diagenesis types of the Cang 1 Member of the Canglangpu Formation in the study area include micritization, recrystallization, cementation, dissolution, compaction, chemical compaction, dolomitization and structural fractures (Zhu, 2014).

Micrization refers to the phenomenon that the edges of carbonate particles are drilled by perforating algae and then filled with micritic calcite (Flügel and Munnecke, 2010). Micritization is weak in the Cang 1 Member of the Canglangpu Formation in the study area. Micritic sleeves formed by micritization are found only in local oolitic limestones. They are usually distributed along the edges of oolitic (Figure 3A).

Recrystallization usually occurs in the internal oolitic of sparry oolitic dolomites and the crystalline dolomite. After recrystallization, the grain size of micrystalline dolomite becomes larger. Furthermore, the micrystalline dolomite is transformed into powder - fine dolomite. Among them, powdery dolomite is dominant (Figure 3B).

The cementation in target clastic rocks is mainly characterized by the circumferential cementation of calcite around terrigenous quartz, lithic debris and feldspar particles (Figure 3C). However, in mixed rocks and carbonate rocks, the cementation mainly develops between oolitic, and the diameter of cementation gradually increases from the edge of oolitic to the pore center. Therefore, the cements are formed at different stages. The first stage was dominated by the horse teeth cements, ctenoid cement and the second stage was dominated by the granular cements (Figure 3D). The second stage of the cement is dyed blue by potassium ferricyanide solution, indicating that the mineral is ankerite, so that the cathode luminescence is not luminescent (Figures 3E–G). The dissolution is significant in the oolitic dolomites (including sparry oolitic dolomites, sand-bearing oolitic dolomites and sandy oolitic dolomites) and fine-grained lithic sandstones in the Cang 1 Member. Intergranular dissolution pores, intra-granular dissolution pores in oolitic dolomites, mold pores and a small number of dissolution caves are developed among oolitic dolomites (Figures 3H–J), while intergranular dissolution pores are developed among detrital particles in fine-grained lithic sandstone, and intra-granular dissolution pores are not developed (Figure 3K). The dissolution of the Cang 1 Member is divided into two stages, include the selective dissolution of fabrics in the meteoric water diagenetic environment and the non-selective dissolution of fabrics in the buried diagenetic environment. In the former, a large number of intergranular dissolved pores, ingranular dissolved pores and a small number of mold pores are formed, while in the latter, a large number of new dissolved pores are formed under the further expansion dissolution of early dissolved pores.

It is found that the compaction is weak in the target carbonate rocks (sparry oolitic dolomite/limestone) and mixed rocks [sand-bearing (sandy) oolitic dolomite]. The (detrital) particles usually show no contact or line contact with each other (Figures 3A,B). However, in clastic rocks (fine-grained lithic sandstone), compaction is strong. Line contact is dominant among the debris particles, followed by point contact and concave-convex contact (Figure 3K). In addition, compaction in the Cang 1 Member also caused ruptures and semi-directional arrangement of oolitic and detrital particles (quartz and debris components) (Figure 3L).

With the increase of compaction, the overburden pressure increases, and the solubility at the contact point of the (detrital) particles increases. Further, chemical compaction occurs, which is manifested as chemical compaction fructures or concave-convex contacts between debris particles (Figures 4A,B).

Strong dolomitization can be observed under the microscope in the Cang 1 Member of the study area. Calcite is mostly metasomatized by dolomite. For example, oolites composed of calcite are usually metasomatized by dolomite and converted to polycrystalline oolites (Figure 4C). By cathodoluminescence observations, it is found that dolomitization of the target layer can be divided into two stages: the first stage occurs in the quasi syngenesis-early stage. Keith and weber (1964) combined C and O isotopes on the basis of Epstein et al., 1953 and Lu (1986) to obtain the empirical formula of paleo-salinity: $Z=2.048 \times (\delta^{13}C+50) + 0.498 \times (\delta^{18}O+50)$. At the same time, on the basis of Urey (1947) and Craig (1965), Keith and Weber (1964) also obtained the empirical formula of paleo-water temperature of Cambrian carbonate rocks: $t=16.9–4.2\ (\delta^{18}O + 0.22)+0.13\ (\delta^{18}O + 0.22)^{2}$. After that, Ma et al., 2022 through the C and O isotope values of the samples in the study area and the above two empirical formulas, it is concluded that the sedimentary period of the first member of the Canglangpu Formation in the study area is hot and the water salinity is high (Tables 2, 3). Lin et al., 2014 and Gu (2020) also found that the palaeoclimate environment in the early Cambrian was hot and dry, which was conducive to the penecontemporaneous dolomitization (capillary concentration or evaporation pump). Combined with the luminescence characteristics of dolomite in the cathodoluminescence thin section, it is found that most of the oolites and the first-stage cements are dim luminescence (Figure 4F), which once again confirms that the first stage dolomitization mainly occurs in the penecontemporaneous period. In addition, the second stage dolomitization mainly occurred in the middle-late stage, which is burial dolomitization, mainly developed at the edge of the first stage cement, and the cathode luminescence of metasomatic dolomite is strong (Figure 4F).

The Canglangpu Formation in the study area was in a stable sedimentary stage from the beginning of deposition to the early Devonian. However, during the Early Devonian-Early Permian periods, due to the influence of the Hercynian Movement, strong tectonic uplift occurred in the central Sichuan region, and a large

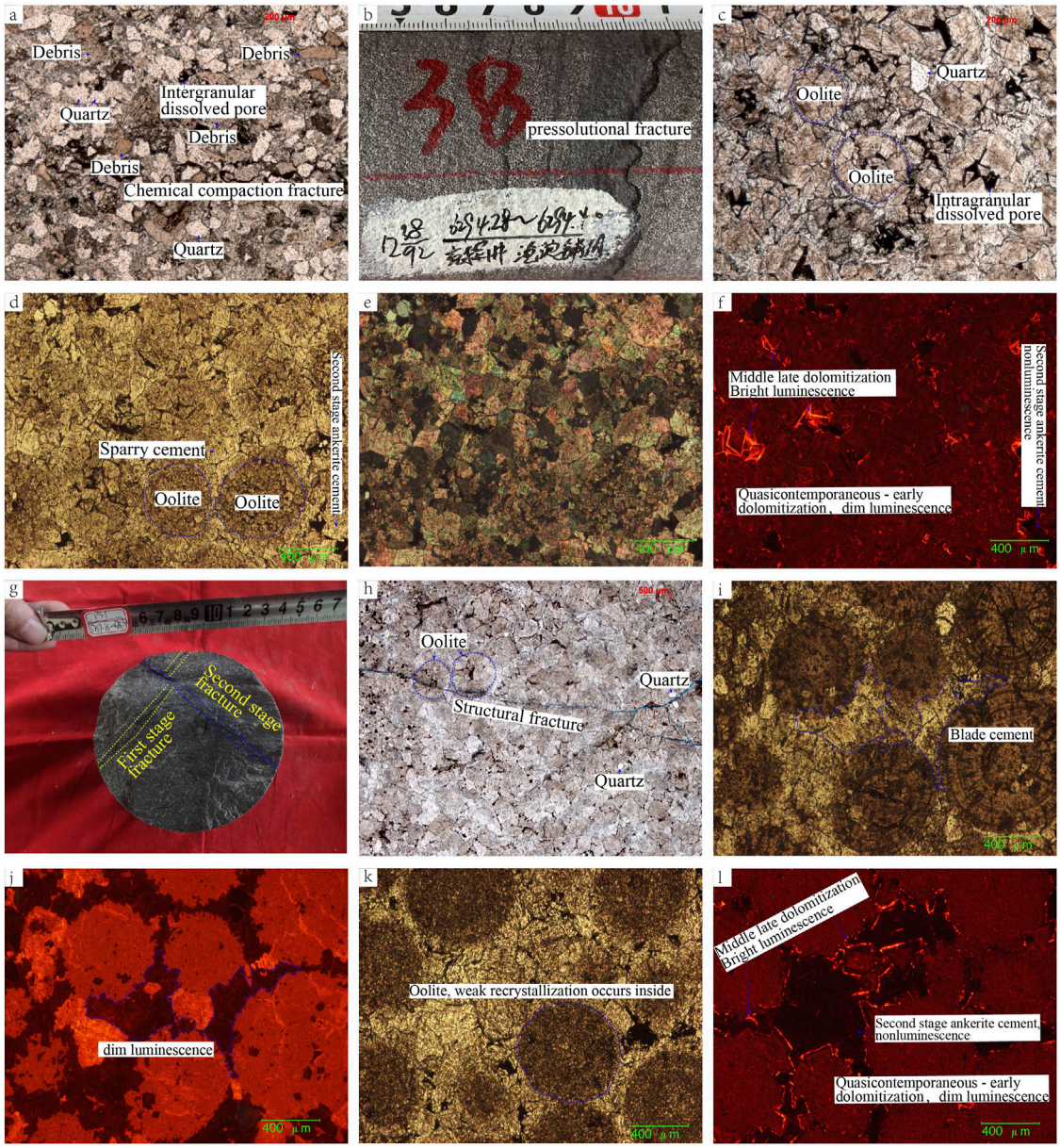

FIGURE 4
Macro and micro features of typical diagenesis observed in the target layer. **(A)** Chemical compaction fracture fully filled with asphalt, fine-grained detrital sandstone, Well PS1, 6783.72 m, single polarized light, dyed cast thin section; **(B)** Chemical compaction fracture fully filled with asphalt, gray sparry oolitic dolomite, 6294.28–6294.40 m, core photo; **(C)** Polycrystalline oolites formed by dolomitization, residual oolitic dolomite, Well CT1, 6273.74 m, single polarized light, dyed cast thin section; **(D)** Sparry oolitic dolomite, Well DB1, 5945.5 m, single polarized light, dyed cast thin section; **(E)** Orthogonal polarized light image of sample d; **(F)** Cathodoluminescence image of sample e; **(G)** The structural dissolution fractures of the first phase are cut by the structural dissolution fractures of the second phase. Gray sand-bearing oolitic dolomite, Well PS1, 6787.15–6787.24 m, core photo; **(H)** Unfilled structural dissolution fractures. Sparry residual oolitic dolomite, Well DB1, 5947.5 m, single polarized light, dyed cast thin section; **(I)** Horses tooth-like cement in seawater diagenetic environment, and its cathodoluminescence characteristic is dim luminescence. Sparry oolitic limestone, Well CT1, 6279.94 m, single polarized light, dyed cast thin section; **(J)** Cathodoluminescence image of sample i; **(K)** Recrystallization in an meteoric water diagenetic environment, and its cathodoluminescence is dim luminescence. Sparry oolitic dolomite, Well DB1, 5944.45 m, single polarized light, dyed cast thin section; **(L)** Cathodoluminescence image of sample k.

number of fractures were formed in the rocks. After the Cretaceous, the margin of the basin was continuously compressed into the basin by the Yanshanian and Himalayan Movements, and the strata were continuously folded and uplifted. Continuous tectonic activities are the direct cause of the formation of fractures in rocks (Mei, 2015; Wang, 2016; Li

10.3389/feart.2022.1059838

TABLE 2 Contents of carbon and oxygen isotopes in the first member of Canglangpu Formation of the Cambrian Series 2 in well JT1, central Sichuan Basin (Ma at el., 2022).

Sample No	Lithology	Isotope	
		δ13CV-PDB	δ18OV-PDB
70-6960m	Powder crystal dolomite	−2.4	−7.7
71-6961m	Powder crystal dolomite	−0.7	−5.9
72-6962m	Powder crystal dolomite	−1	−6.3
73-6963m	Powder crystal dolomite	−3.1	−9.3
74-6964m	Powder crystal dolomite	−1.6	−6.3
75-6965m	Powder crystal dolomite	−1.3	−5.9
76-6966m	Powder crystal dolomite	−3.4	−9.3
77-6967m	Mudstone	−2.5	−8.8
78-6968m	Oolitic dolomite	−2.9	−8.9
79-6969m	Calcareous mudstone	−0.7	−6.5
80-6970m	Powder crystal dolomite	−1.1	−7.1
81-6971m	Powder crystal dolomite	−0.6	−6.9
82-6972m	Powder crystal dolomite	−0.4	−6.2
83-6973m	Argillaceous dolomite	−0.8	−6.9
85-6975m	Powder crystal dolomite	−0.9	−7.1
86-6976m	Powder crystal dolomite	−1.4	−7.1
87-6977m	Argillaceous dolomite	−0.7	−-7.2
88-6978m	Argillaceous dolomite	−1.3	−7.8
89-6979m	Argillaceous dolomite	−0.9	−7.5
90-6980m	Argillaceous dolomite	−1	−8.1
91-6981m	Powder crystal dolomite	−0.8	−7.3
93-6983m	Oolitic dolomite	−0.9	−7.6
94-6984m	Oolitic dolomite	−0.8	−7.4
1-6985m	Oolitic dolomite	−0.6	−6.9
3-6987m	Oolitic dolomite	−0.6	−7
4-6988m	Oolitic dolomite	−0.8	−7
5-6989m	Oolitic dolomite	−0.8	−7.3
6-6990m	Oolitic dolomite	−1.6	−8.6
7-6991m	Oolitic dolomite	−1.8	−7.7
8-6992m	Oolitic dolomite	−1.1	−7.4
10-6994m	Calcareous mudstone	−1.9	−9.6
11-6995m	Calcareous mudstone	−2	−9.5
12-6996m	Argillaceous limestone	−1.8	−9.9
13-6997m	Argillaceous limestone	−0.9	−8.5
17-7001m	Oolitic limestone	−1.7	−9.7
18-7002m	Oolitic limestone	−1.9	−9.1
19-7003m	Oolitic limestone	−1.5	−8.4
20-7004m	Oolitic limestone	−2.1	−9.8
21-7005m	Oolitic limestone	−1.5	−8.9
23-7007m	Oolitic limestone	−1.3	−9.2
24-7008m	Oolitic limestone	−1.4	−9.5
25-7009m	Oolitic limestone	−1.2	−10
38-7022m	Oolitic limestone	−0.9	−10
40-7024m	Oolitic limestone	−1.4	−9.2
41-7025m	Sandy limestone	−1.3	−8.4

(Continued on following page)

TABLE 2 (*Continued*) Contents of carbon and oxygen isotopes in the first member of Canglangpu Formation of the Cambrian Series 2 in well JT1, central Sichuan Basin (Ma at el., 2022).

Sample No	Lithology	Isotope	
		δ13CV-PDB	δ18OV-PDB
42-7026m	Sandy limestone	−1.5	−9.3
43-7027m	Sandy limestone	−1.5	−8.2
44-7028m	Sandy limestone	−2.1	−9
46-7030m	Sandy limestone	−1.6	−8.8
48-7032m	Sandy limestone	−2.1	−9.2
50-7034m	Sandy limestone	−1.4	−9
52-7036m	Sandy limestone	−2.1	−9.5
53-7037m	Oolitic limestone	−1.5	−8.7
55-7039m	Oolitic limestone	−2.1	−10

et al., 2019; Li, 2022b; Li J. et al., 2022c; Li H. et al., 2022d). The structural fracturess of the target layer mainly occurred in the Hercynian and Yanshanian-Himalayan periods. Fractures generated during the Yanshanian-Himalayan period cut the fractures generated during the Hercynian period (Figure 4G). Moreover, the fractures experienced strong dissolution at the later stage of deposition, and then the structural dissolution fractures were formed. This kind of structural dissolution fractures are mostly filled with asphalt, dolomite and pyrite, and a small amount is not filled (Figures 4G,H).

4.2.2 Diagenetic environment and stages

Diagenetic environment refers to the physical and chemical conditions that cause changes in the properties of sediments and early sedimentary rocks (Zhou and Zhang, 1993). According to the properties and occurrence states of diagenetic fluids (pore water), the diagenetic environments of the Cang 1 Member can be divided into seawater diagenetic environment, meteoric water diagenetic environment, evaporative seawater diagenetic environment and buried diagenetic environment (Moore, 1989; Zhou et al., 1993). According to the luminous characteristics of each component in the cathodoluminescent thin section of the study area, the types and characteristics of diagenesis, it is found that the first member of Canglangpu Formation has experienced seawater diagenetic environment, meteoric water diagenetic environment, evaporation seawater diagenetic environment and burial diagenetic environment. The diagenetic stages include syngenetic stage, quasi syngenetic stage, early diagenetic stage and middle-late diagenetic stage.

4.2.2.1 Seawater diagenetic environment (syngenetic stage)

The seawater diagenetic environment is the early external environment of marine carbonate rocks after deposition (Hang, 2010). Typical diagenetic types in seawater diagenetic environments include micritization, equithick fibrous ring-edge cementation, disorderly needle-like cementation, bladed cementation and fibrous calcite cementation, etc. (Huang., 2010; Qiang., 1998). A large number of horse tooth cements and slight micritic sleeve were formed in the Cang 1 Member under seawater diagenetic conditions (Figure 3A). And its cathodoluminescence tests showed dim luminescence (Figures 4I,J).

4.2.2.2 Meteoric water diagenetic environment (quasi-syngenetic stage)

The meteoric water diagenetic environment refers to the mixed environment between the surface and freshwater and seawater (Huang, 2010). In meteoric water environment, the pores are filled with atmospheric water and air. The pore fluid is rich in CO_2 and has strong solubility. The selective dissolution of the fabric promotes the formation of dissolved pores and mold pores. At the same time, strong cementation leads to the formation of crescentic and gravity cementation. The target layer mainly showed weak recrystallization (Figure 3D) and selective dissolution of the fabric in the meteoric water diagenetic environment. The former showed dim luminescence under the cathodoluminescence tests (Figures 4K,L), while the latter showed the formation of a large number of intragranular dissolved pore and a small number of mold pores (Figures 3H,I).

4.2.2.3 Evaporative seawater diagenetic environment (quasi-syngenetic stage)

Evaporative seawater diagenetic environment refers to the environment with dry climate and strong evaporation. The early Canglangpu Formation was deposited in an arid and hot paleoclimatic environment (Lin et al., 2014; Gu, 2020). In this environment, calcite is metasomatized by dolomite, and the

TABLE 3 Date of paleotemperature and paleo-salinity of the first member of Canglangpu Formation of the Cambrian Series 2 from Well JT1 in central Sichuan Basin (Ma at el., 2022).

Sample No	Paleo-salinity index Z	Uncorrected paleo-salinity S/‰	Corrected paleo-salinity S/‰	Paleo-water temperature/°C
70-6960m	119	27.1	34.1	18.9
71-6961m	123	28.9	35.9	11.6
72-6962m	122	28.5	35.5	13.1
73-6963m	116	25.5	32.5	26.2
74-6964m	121	28.5	35.5	13.1
75-6965m	122	28.9	35.9	11.6
76-6966m	116	25.5	32.5	26.2
77-6967m	118	26	33	23.9
78-6968m	117	25.9	32.9	24.3
79-6969m	123	28.3	35.3	13.9
80-6970m	122	27.7	34.7	16.4
81-6971m	123	27.9	34.9	15.6
82-6972m	123	28.6	35.6	12.8
83-6973m	122	27.9	34.9	15.6
85-6975m	122	27.7	34.7	16.4
86-6976m	121	27.7	34.7	16.4
87-6977m	122	27.6	34.6	16.8
88-6978m	121	27	34	19.4
89-6979m	122	27.3	34.3	18.1
90-6980m	121	26.7	33.7	20.7
91-6981m	122	27.5	34.5	17.2
93-6983m	122	27.2	34.2	18.5
94-6984m	122	27.4	34.4	17.7
1-6985m	123	27.9	34.9	15.6
3-6987m	123	27.8	34.8	16
4-6988m	122	27.8	34.8	16
5-6989m	122	27.5	34.5	17.2
6-6990m	120	26.2	33.2	22.9
7-6991m	120	27.1	34.1	18.9
8-6992m	121	27.4	34.4	17.7
10-6994m	119	25.2	32.2	27.6
11-6995m	118	25.3	32.3	27.2
12-6996m	119	24.9	31.9	29.1
13-6997m	121	26.3	33.3	22.5
17-7001m	119	25.1	32.1	28.1
18-7002m	119	25.7	32.7	25.3
19-7003m	120	26.4	33.4	22
20-7004m	118	25	32	28.6
21-7005m	120	25.9	32.9	24.3
23-7007m	120	25.6	32.6	25.7
24-7008m	120	25.3	32.3	27.2
25-7009m	120	24.8	31.8	29.6
38-7022m	120	24.8	31.8	29.6
40-7024m	120	25.6	32.6	25.7
41-7025m	120	26.4	33.4	22
42-7026m	120	25.5	32.5	26.2

(Continued on following page)

TABLE 3 (*Continued*) Date of paleotemperature and paleo-salinity of the first member of Canglangpu Formation of the Cambrian Series 2 from Well JT1 in central Sichuan Basin (Ma at el., 2022).

Sample No	Paleo-salinity index Z	Uncorrected paleo-salinity S/‰	Corrected paleo-salinity S/‰	Paleo-water temperature/°C
43-7027m	120	26.6	33.6	21.1
44-7028m	119	25.8	32.8	24.8
46-7030m	120	26	33	23.9
48-7032m	118	25.6	32.6	25.7
50-7034m	120	25.8	32.8	24.8
52-7036m	118	25.3	32.3	27.2
53-7037m	120	26.1	33.1	23.4
55-7039m	118	24.8	31.8	29.6

metasomatized dolomite has dim luminescence under the cathodoluminescence tests (Figures 4F,L).

4.2.2.4 Shallow burial diagenetic environment (early diagenetic stage)

The temperature and pressure in the shallow buried diagenetic environment are close to the surface conditions, and the diagenetic fluids are mainly atmospheric water, seawater and mixed water between them (Huang, 2010). Usually, the diagenetic temperature is lower than 85°C, and the rock is mainly affected by mechanical compaction. Under the overburden load condition, the rock particles will be broken and deformed, and there will be concave-convex contact between the particles (Figure 3L).

4.2.2.5 Medium-deep burial diagenetic stage (middle-late diagenetic stage)

In middle-deep buried diagenetic environments, diagenetic fluids are not directly affected by atmospheric water and sea water, and free oxygen almost does not exist. When carbonate rocks are in medium-deep burial environment, chemical compaction occurs (Huang, 2010). Chemical compaction fractures can be observed for the Cang1 Member in a medium-deep burial diagenetic environment (Figures 4A,B). In addition, two stages of cementation were observed. Strong dolomitization occurred at the edge of the first-stage cement, which manifested as strong luminescence under cathodic luminescence (Figures 4F,L). However, the second stage is the granular cementation of ankerite, which shows no luminescence (Figures 3E–G).

5 Discussion

5.1 Analysis of diagenetic sequence

The Canglangpu Formation conformable contact with the lower Qiongzhusi and the overlying Longwangmiao Formations. Therefore, the burial history of the Qiongzhusi Formation was similar to that of the Canglangpu Formation (Figure 5).

It can be seen from Figure 5 that both the Canglangpu and Qiongzhusi Formations experienced five sedimentary evolution stages, including three settlement-sedimentation stages and two uplift stages. They are stable settlement-sedimentation, stable uplift, rapid settlement-sedimentation, rapid settlement-sedimentation and rapid uplift, respectively. Therefore, from the early Canglangpu Formation to the early Devonian, the Canglangpu Formation was continuously deposited to a buried depth of 2000 m. After that, tectonic uplift occurred, and by the late Carboniferous, the average buried depth was only 800 m. Subsequently, the burial depth of the Canglangpu Formation increased continuously, and another uplift occurred in the early to middle Cenozoic, but the whole Canglangpu Formation was still in a deep burial environment.

According to the types and characteristics of diagenesis, regional tectonic setting, diagenetic environment analysis and burial history construction of the Cang1 Member in the study area, it is believed that the Cang 1 Member in the study area has experienced three major diagenetic stages, include syngeneic and quasi-syngeneic diagenetic stage, early diagenetic stage and middle-late diagenetic stage (Figure 5). According to Figure 5, tectonic uplift occurred in the Canglangpu Formation in the early Devonian and early Cenozoic, but the strata were not uplifted to the surface, so they did not undergo the epigenetic stage. The constructed diagenetic sequence of the Cang1 Member in the study area is shown in Figure 6.

5.2 Influence of diagenesis on pore development

For old strata with complex geological development history, the fundamental factor affecting porosity is no longer the original

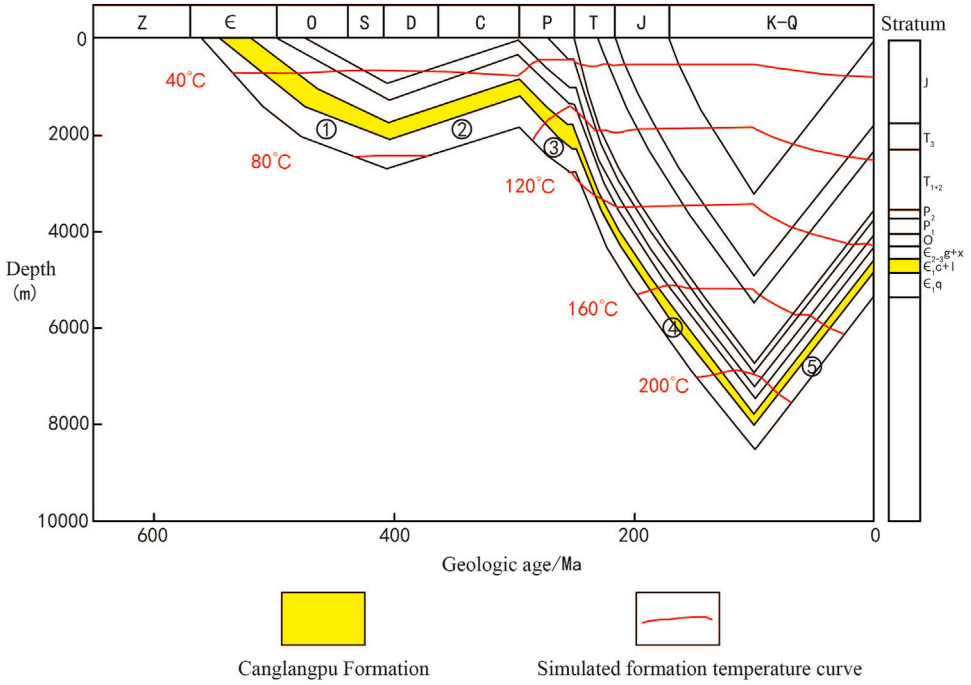

FIGURE 5
Burial history of the Qiongzhusi Formation in Well GS 17 in the Central Sichuan Paleo-uplift (modified from reference Yang et al., 2020). ①: The first stable settlement-sedimentation period; ②: The first stable uplift period; ③: The second rapid settlement-sedimentation period; ④: The third rapid settlement-sedimentation period; ⑤ The second rapid uplift period.

sedimentary structure, but the modification of diagenesis in the late sedimentary period (Shi et al., 2010). The diagenesis of the first member of Canglangpu Formation in the study area plays a key role in the development of pores, includes diagenesis that facilitates pore development, preservation and diagenesis that reduces surface porosity.

5.2.1 Diagenesis that facilitates to pore development and preservation

Diagenesis beneficial to pore development and preservation in the study area mainly includes Structural fracture, dissolution, dolomitization and the first stage cementation.

Structural fracture: Influenced by the Hercynian, Yanshanian and Himalayan Movements, a large number of tectonic fractures occurred in the Cang 1 Member of the Canglangpu Formation in the study area (Mei, 2015; Wang, 2016). Structural fractures are conducive to the flow of acidic formation water, promote dissolution, expand the original pores and form new dissolution pores. At the same time, when acidic formation water flows through structural fractures, the fractures will also be widened by dissolution, forming structural dissolution fractures, which is more conducive to the development of rock pores. Thus, the more developed the structural dissolution fractures, the more favorable the development of pores (Figure 7).

Dissolution: In the quasi-syngenetic meteoric water diagenetic environment, the selective dissolution of the fabric results in the formation of a large number of intra-granular dissolved pores, intergranular dissolved pores, and mold pores. Furthermore, under the background of the formation of a large number of dissolution pores in the quasi-syngenesis period, acidic fluids and hydrothermal fluids in the burial period can flow better and react adequately with rocks. At this time, the pore size of the early dissolved pores is expanded, and some new intergranular dissolved pores, intra-granular dissolved pores and vugs are formed.

Dolomitization: The early Canglangpu Formation was deposited in an arid and hot paleoclimatic environment (Lin et al., 2014; Gu, 2020). Intense dolomitization results in a large amount of calcite metasomatized by dolomite to form dolomite, calcite dolomite and dolomitic limestone. After entering the burial stage, the dolomite formed by early dolomitization has stronger compressive resistance during the burial process, and the original and the secondary dissolution pores formed in the early stage can be well protected. With the increase of burial depth, when the burial depth is more than 2000 m (the average burial depth of the Cang1 Member in the study area is more than 5000 m), burial dolomitization will cause the decrease of solid phase volume and the increase of pore size (Joachim et al., 1994;

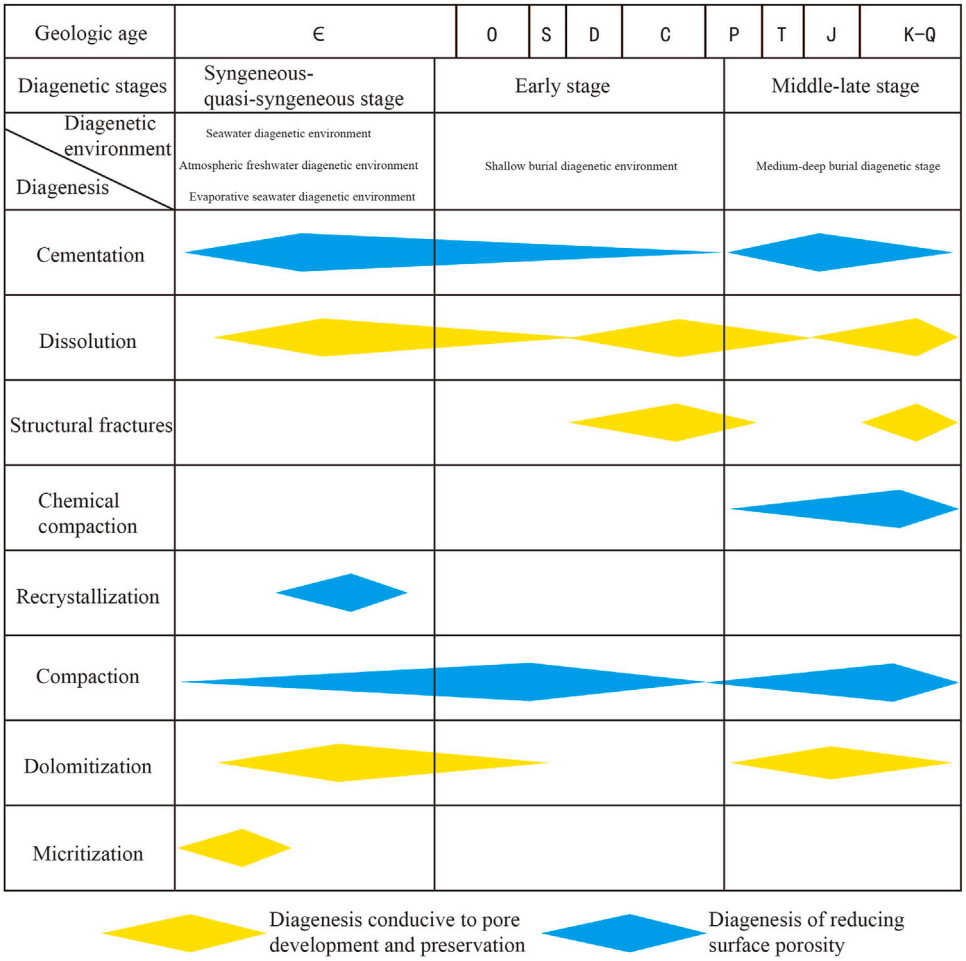

FIGURE 6
Construction results of the diagenetic sequence of the Cang 1 Member of the Canglangpu Formation.

Huang, 2010; Zhou et al., 2015; Xie et al., 2018). It can be found from Figure 7 that the oolitic dolomite at the middle and upper part of the coring section (6262–6275 m) is completely dolomitized, calcite is completely metasomatized by dolomite, and its pores are relatively developed as a whole; However, the oolitic dolomite at 6288–6301 m in the middle and lower part is not completely dolomitized, containing a certain calcite, and its pores are poorly developed as a whole (Figure 7).

The first stage of cementation: in the submarine diagenesis environment and the meteoric water diagenesis environment, the drusy cement, the dentate cement and the leaf-like cement can support the pores (Shun, 2021) and have a certain protective effect on the pores. In summary, structural fracture, dissolution, dolomitization and first-stage cementation can not only protect pre-pores and form new secondary pores, but also improve pore throats and promote pore development (Figures 8A–C).

Supplement: the degree of compaction is reflected by the particle contact relationship, 0–1 indicates that the particles are mainly non-contact with a small amount of point contact; 1-2 indicates that the particles are mainly in point contact with a small amount of line contact; more than or equal to 2 indicates that the particles are mainly in line contact with a small amount of suture contact. GR: natural gamma ray; Rt: true formation resistivity; Rxo: flushed zone formation resistivity.

5.2.2 Diagenesis that reduces surface porosity

The diagenesis of reducing pore surface porosity in the study area mainly includes the second stage cementation, compaction and chemical compaction.

Second stage cementation: it is mainly granular ankerite cementation in the burial period. With the progress of the second stage cementation, the content of cement increases

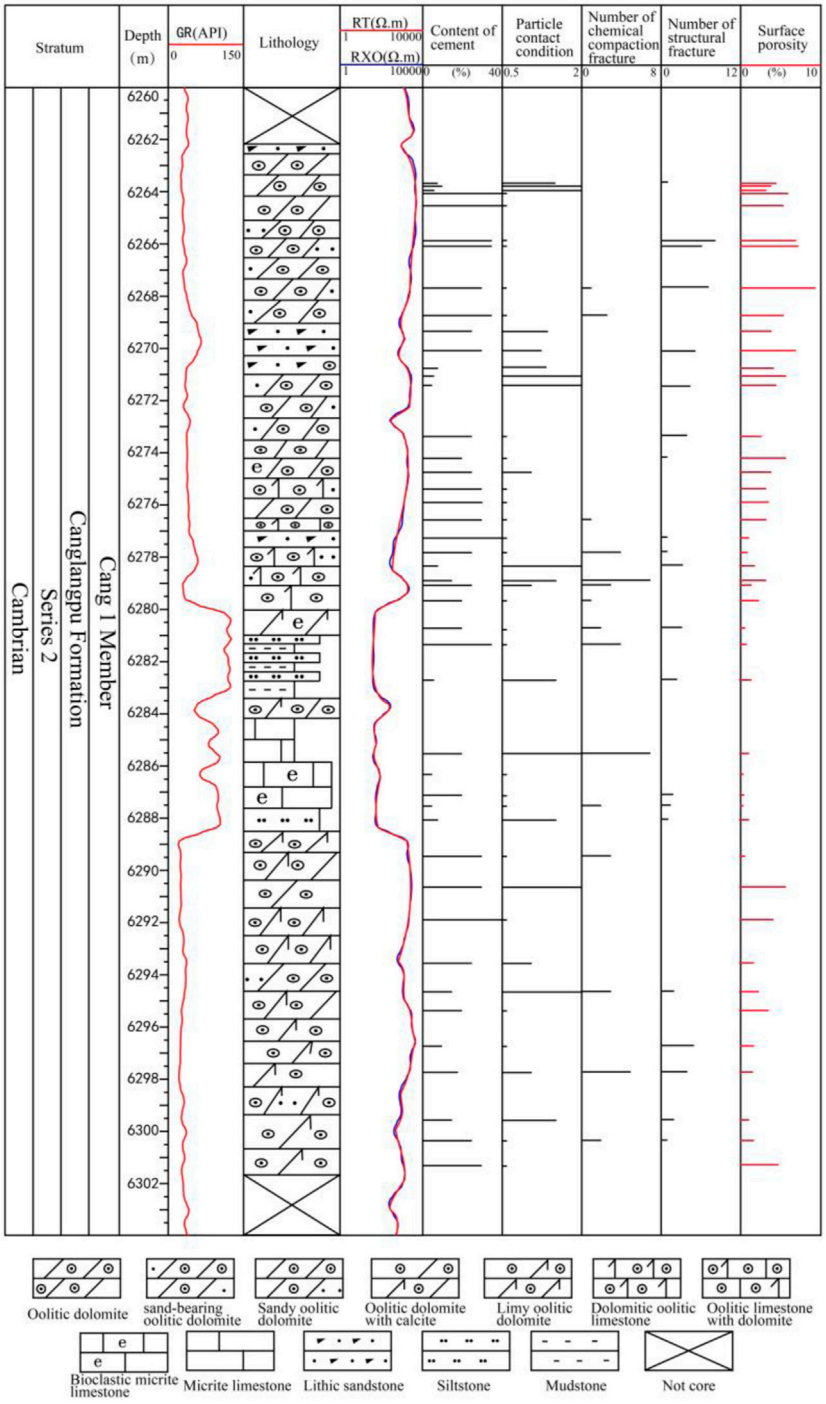

FIGURE 7
Histogram of diagenesis in coring section of well CT1.

continuously, so that the pores are gradually filled, and the pore size of the pores is gradually reduced or even fully filled, which is not conducive to the development of pores.

Compaction: the compaction in the study area is mainly controlled by two aspects. One is the overlying pressure exerted by the overlying sediments, and the other is the

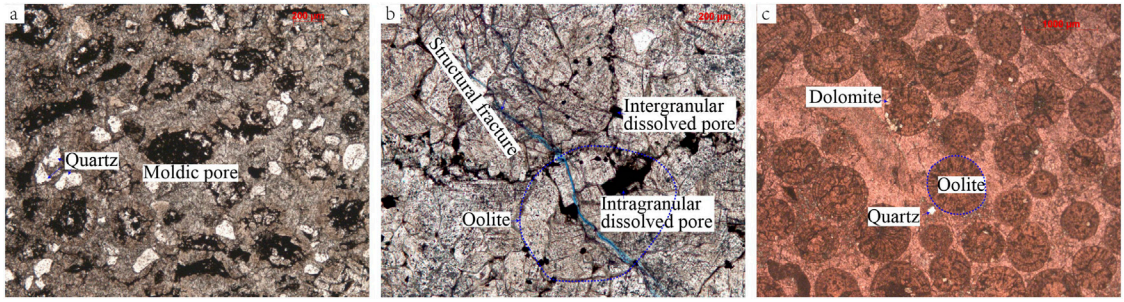

FIGURE 8
Effect of diagenesis on pore development. **(A)** Strong dolomitization and dissolution, and weak compaction. Sparry oolitic dolomite, Well CT1, 6266.42 m, single polarized light, dyed cast thin section; **(B)** Strong structural fracture and dolomitization, and pores are relatively developed. Sparry oolitic dolomite, Well DB1, 5947.5 m, single polarized light, dyed cast thin section; **(C)** Extremely underdeveloped pores, due to strong cementation, weak dolomitization, dissolution, and structural rupture. Sparry oolitic limestone, Well Chongtan 1, 6279.94 m, single polarized light, dyed cast thin section.

properties of the sediments themselves, including the composition of the sediments, the content, sorting, and rounding of rigid particles. The (detrital) particles in the target layer in the study area are mainly include oolitic, quartz and rock debris, which have relatively little protective effect on the rock pores. The pressure exerted by overlying sediments is a key factor affecting the development of pores in the study area. With the increase of burial depth and overburden pressure, the pore size gradually decreases or even disappears, which is not conducive to the development of the rock pores. Thus, the compaction of rock is enhanced and the development of rock pores is weakened (Figure 7).

Chemical compaction: the chemical compaction of the target layer in the study area occurred on the basis of strong compaction. It can further destroy the pores and eventually lead to the reduction of the pore size inside the rocks.

Based on this study, the second stage cementation, compaction and chemical compaction are not conducive to the development of pores. Therefore, a weak diagenetic coupling of cementation, compaction and chemical compaction is favorable for the development of pores (Figures 8A–C).

6 Conclusion

(1) In this paper, taking the Cang 1 Member of the Canglangpu Formation of the Cambrian Series 2 in the north part of the central Sichuan Basin as an example, the diagenesis and its influence on pores are systemically studied based on the observations and identifications of cores, cast and cathodoluminescence thin sections.

(2) The rock types of the Cang 1 Member of the Canglangpu Formation are mainly include sand-bearing oolitic dolomite, sandy oolitic dolomite, sparry oolitic dolomite and fine-grained lithic sandstone. At the same time, the Cang 1 Member of the Canglangpu Formation in the study area has experienced five types of diagenetic environments, including seawater, meteoric water, evaporative seawater, shallow burial, and medium-deep burial diagenetic environments.

(3) The main diagenetic processes under different diagenetic environment conditions are cementation, dissolution, compaction, chemical compaction, dolomitization and structural fractures. According to the analysis, fabric-selective dissolution in meteoric water diagenetic environment, dolomitization in evaporative seawater environment, the first stage cementation in submarine diagenetic environment and meteoric water diagenetic environment, such as drusy cementation, dentate cementation, leaf-like cementation and non-fabric-selective dissolution, dolomitization and structural fractures in buried diagenetic environment is beneficial to the development of the pores. However, the second stage cementation, compaction and chemical compactionin medium-deep burial environments, are unfavorable for the development of the pores.

Data availability statement

The original contributions presented in the study are included in the article/Supplementary Material; further inquiries can be directed to the corresponding author.

Author contributions

BZ and HQ are responsible for the idea and writing of this paper, XZ and QH are responsible for the data sorting, RZ,

LZ, YZ, ZM, QM, and HA are responsible for sample collection.

Funding

This research was financially supported by the National Natural Science Foundation of China (41702163, 41702122) and the Science and Technology Cooperation Project of the CNPC-SWPU Innovation Alliance (No. 2020CX010301).

Conflict of interest

The authors RZ, YZ, QM, and HA were employed by the company Exploration Department of PetroChina Southwest Oil and Gasfield Company. The authors LZ and ZM were employed by the company Central Sichuan Oil and Gas Mine of PetroChina Southwest Oil and Gas Field Company. The author YP was employed by CNPC Chuanqing Drilling Engineering Company Limited.

The remaining authors declare that the research was conducted in the absence of any commercial or financial relationships that could be construed as a potential conflict of interest.

Publisher's note

All claims expressed in this article are solely those of the authors and do not necessarily represent those of their affiliated organizations, or those of the publisher, the editors and the reviewers. Any product that may be evaluated in this article, or claim that may be made by its manufacturer, is not guaranteed or endorsed by the publisher.

References

Craig, H. (1965). The measurement of oxygen isotope paleotemperatures.Stable isotopes in oceanographic studies and Paleotemperatures.Piza:consiglio nazionale delle richerche. *Lab. Geol. Nucl.* 3, 23.

Dong, G., Chen, H., and He, Y. (2007). Some problems on the study of the mixed siliciclastic-carbonate sediments. *Adv. Earth Sci.* 22 (9), 931–939.

Dong, T., Li, X., and Peng, C. (2021). "Reservoir pre-diction of the cambrian Canglangpu Formation in the xichongarea of central and northern sichuan," in Proceedings of the Geophysical Exploration Technology Seminar of China Petroleum Society, Chengdu, China, September 27, 2021, 768–771. doi:10.26914/c.cnkihy.2021.014594

Epstein, S., Buchsbaum, R., Lowenstam, H., and Urey, H. C. (1953). Revised carbonate-water isotopic temperature scale. *Geol. Soc. Am. Bull.* 64 (11), 1315–1326. doi:10.1130/0016-7606(1953)64[1315:RCITS]2.0.CO;2

Flügel, E., and Munnecke, A. (2010). *Microfacies of carbonate rocks: Analysis, interpretation and application*. Berlin, Germany: Springer, 1–5. ISBN:978-3-642-03795-5.

Gu, Z. (2020). *Sedimentary characteristics and petroleum geological significance of Cambrian gypsum salt rocks in Sichuan basin and its surrounding areas*. Jingzhou, China: Yangtze University. doi:10.26981/d.cnki.gjhsc.2020.000593

Hu, D., Wang, L., and Huang, R. (2021). Petroleum exploration history and enlightenment in Sichuan Basin: A case study on sinopec exploration areas. *Xinjiang Pet. Geol.* 42 (3), 283–290. doi:10.7657/XJPG20210304

Huang, S. (2010). *Carbonate diagenesis*. Beijing, China: Geologyical Publishing House, 1–4. ISBN:978-7-116-06938-1.

Joachim, E., Amthor, E. W., and Mountjoy, H. G. (1994). Machel. Regional-scale porosity and permeability variations in Upper Devonian Leduc buildups; implications for reservoir development and prediction in carbonates. *GeoScienceWorld* 78 (10). doi:10.1306/A25FF215-171B-11D7-8645000102C1865D

Keith, M., and Weber, J. (1964). Carbon and oxygen isotopic composition of selected limestones and fossils. *Geochim. Cosmochim. Acta* 28, 1787–1816. doi:10.1016/0016-7037(64)90022-5

Li, H. (2022b). Research progress on evaluation methods and factors influencing shale brittleness: A review. *Energy Rep.* 8, 4344–4358. doi:10.1016/j.egyr.2022.03.120

Li, H., Tang, H. M., Qin, Q. R., Zhou, J. L., Qin, Z. J., Fan, C. H., et al. (2019). Characteristics, formation periods and genetic mechanisms of tectonic fractures in the tight gas sandstones reservoir: A case study of xujiahe Formation in YB area, Sichuan Basin, China. *J. Pet. Sci. Eng.* 178, 723–735. doi:10.1016/j.petrol.2019.04.007

Li, H., Zhou, J. L., Mou, X. Y., Guo, H. X., Wang, X. X., An, H. Y., et al. (2022d). Pore structure and fractal characteristics of the marine shale of the longmaxi Formation in the changning area, southern Sichuan Basin, China. *Front. Earth Sci.* 10, 1018274. doi:10.3389/feart.2022.1018274

Li, J., Li, H., Yang, C., Wu, Y. J., Gao, Z., and Jiang, S. L. (2022c). Geological characteristics and controlling factors of deep shale gas enrichment of the Wufeng-Longmaxi Formation in the southern Sichuan Basin, China. *Lithosphere* 2022, 4737801. doi:10.2113/2022/4737801

Lin, L., Hao, Q., and Yu, Y. (2014). Development characteristics and sealing effectiveness of Lower Cambrian gypsum rock in Sichuan Basin. *Acta Petrol. Sin.* 30 (3), 718–726.

Li, Q., Bao, Z., and Xiao, Y. (2021b). Research advances and prospect of mixed deposition. *Acta Sedimentol. Sin.* 39 (1), 153–167. doi:10.14027/j.issn.1000-0550.2020.140

Li, S., Jiang, P., and Liu, L. (2022a). Seismic response characteristics and distribution law of carbonate shoals of Cang-langpu Formation in Gaoshiti-Moxi area, Sichuan Basin. *Lithol. Reserv.* 34 (4), 22–31. doi:10.12108/yxyqc.20220403

Li, Y., Chen, Y., and Yan, W. (2021a). Research on sedimentary evolution characteristics of cambrian Canglangpu formation, Sichuan Basin. *Nat. Gas. Geosci.* 32 (9), 1334–1346. doi:10.11764/j.issn.1672-1926.2021.03.010

Lu, W. (1986). *Stable isotope geochemistry*. Sichuan Chengdu, China: Chengdu Institute of Geology Press, 1–334.

Ma, S., Xie, W., and Yang, W. (2021). Lithofacies and paleogeography of the lower Canglangpu Formation of the lower cambrian in Sichuan Basin and its periphery. *Nat. Gas. Geosci.* 32 (9), 1324–1333. doi:10.11764/j.issn.1672-1926.2021.03.011

Ma, T., He, Y., and Zhu, L. (2022). Carbon and oxygen isotope characteristics of lower Canglangpu Formation of lower cambrian in central sichuan and the geological significance. *J. Chengdu Univ. Technol. Technol. Ed.* 1–17.

Mei, Q. (2015). *Tec-tonic evolution and formation mechanism of Leshan-Longnüsi paleo-uplift, Sichuan Basin*. Beijing, China): Beijing:China University of Geosciences, 1–4.

Moore, C. H. (1989). *Carbonate diagenesis and porosity*. Amsterdam, Netherlands: Elsevier, 45–47. ISBN: 0-444-87415-1.

Mount, J. F. (1984). Mixing of siliciclastic and carbonate sediments in shallow shelf environments. *Geol.* 12 (7), 432–435. doi:10.1130/0091-7613(1984)12<432:mosacs>2.0.co;2

Peng, J., Chu, J., and Chen, Y. (2020). Sedimentary characteristics of lower cambrian Canglangpu Formation in GaoshitiMoxi area, Sichuan Basin. *Lithol. Reserv.* 32 (4), 12–22. doi:10.12108/yxyqc.20200402

Qiang, Z. (1998). *Carbonate reservoir geology*. DongYing, China: Petroleum University Publishing House, 18–23. ISBN:7-5636-1130-4.

Sha, Q. (2001). Discussion on mixing deposit and Hunji rock. *J. Palaeogeogr.* 3 (3), 63–66.

Shi, G., Tian, J., and Wu, Y. (2010). Lower Paleozoic Carbonate diagenesis feature and controlling over reservoirs in southern North China. *Geol. Sci. Technol. Inf.* 29 (2), 10–15.

Shun, Y. (2021). *Diagenesis characteristics of jurassic reservoir and its influence on reservoir in moxizhuang yongjin area, junggar basin*. Kirkland, DC: Northwest University, 1–5. doi:10.27405/d.cnki.gxbdu.2021.001052

Urey, H. (1947). The thermodynamic properties of isotopic substances. *J. Chem. Soc.*, 562–581. doi:10.1039/JR9470000562

Wang, C. (2016). *The study on structure feature of Longwangmiao Formation in gaoshiti-moxi area, Sichuan Basin*. Chengdu, China: Chengdu University of Technology, 23–25.

Wang, L., Su, S., and Ma, Z. (2022). Sedimentary characteristics of cambrian Canglangpu Formation in central SichuanBasin. *Lithol. Reserv.* 34 (6), 19–31. doi:10.12108/yxyqc.20220602

Wang, W., Fan, Y., and Lai, Q. (2018). A new understanding ofdolomite distribution in the Lower Cambrian Canglangpu for mation of Sichuan Basin: Implication for petroleum geology. *Nat. Gas Explor. Dev.* 41 (1), 1–7. doi:10.12055/gaskk.issn.1673-3177.2018.01.001

Wang, Z., Jiang, H., Wang, T., Lu, W., Gu, Z., Xu, A., et al. (2014). Paleo-geomorphology formed during Tongwan tectonization in Sichuan Basin and its significance for hydrocarbon accumulation. *Petroleum Explor. Dev.* 41 (3), 338–345. doi:10.1016/s1876-3804(14)60038-0

Wen, J., Peng, J., and Chen, Y. (2020). Study on sequencestratigraphy of Canglangpu Formation in the central-northernSichuan asin. *Fault-Block Oil Gas Field* 27 (4), 424–431. doi:10.6056/dkyqt202004004

Xie, X., Ye, M., and Xu, C. (2018). High quality reservoirs characteristics and forming mechanisms of mixed siliciclastic-carbonate sediments in the bozhong sag, bohai bay basin. *Earth Sci.* 43 (10), 3526–3539. doi:10.3799/dqkx.2018.277

Yan, W., Luo, B., Zhou, G., Chen, Y., Zhong, Y., Li, K., et al. (2021). Natural gas geology andexploration direction of the Cambrian lower Canglangpu memberin central Sichuan paleo-uplift, Sichuan Basin, SW China. *Petroleum Explor. Dev.* 48 (2), 337–353. doi:10.1016/s1876-3804(21)60027-7

Yan, W., Zhong, Y., and Zhou, G. (2020). Lithofacies paleo geography features of the Lower Cambrian Canglangpu Formationin Sichuan Basin and their control on reservoir development. *Nat. Gas Explor. Dev.* 43 (4), 22–32. doi:10.12055/gaskk.issn.1673-3177.2020.04.003

Yang, C., and Sha, Q. (1990). Sedimentary environmentof the Middle Devonian Qujing Formation, Qujing, Yunnan province:A kind of mixing sedimentation of terrigenous clastics andcarbonate. *Acta Sedimentol. Sin.* 8 (2), 59–66.

Yang, C., Wen, L., and Wang, T. (2020). Timing of hydrocarbon accumulation for paleo-oil reservoirs in anyue gas field in chuanzhong uplift. *Oil Gas Geol.* 41 (3), 492–502. doi:10.11743/ogg20200306

Yue, H., Zhao, L., and Yang, Y. (2020). Great discovery of oiland gas exploration in cambrian Canglangpu Formation of the Sichuan Basin and its implications. *Nat. Gas. Ind.* 40 (11), 11–18. doi:10.3787/j.issn.1000-0976.2020.11.002

Zhang, J., and Ye, H. (1989). A study on carbonate and siliciclastic mixed sediments. *J. Chengdu Univ. Technol.* 16 (2), 87–92.

Zhang, X. (2000). Classification and origin of mixosed mentite. *Geol. Sci. Technol. Inf.* 19 (4), 31–34.

Zhou, J., Xu, C., Yao, G., Yang, G., Zhang, J., Hao, Y., et al. (2015). Genesis and evolution of lower cambrian Longwangmiao Formation reservoirs, Sichuan Basin, SW China. *Petroleum Explor. Dev.* 42 (2), 175–184. doi:10.1016/s1876-3804(15)30004-5

Zhou, S., and Zhang, X. (1993). Diagenetic environment and pore evolution of carbonate rocks. *Oil & Gas. Geol.* 14 (3), 215–222+261.

Zhu, X. (2014). *Sedimentary petrology*. Fourth Edition. BeiJing, China: Petroleum Industry Publishing House, 56–59. ISBN:978-7-5021-6755-4.